

# Transient aggregation of ubiquitinated proteins during dendritic cell maturation

Hugues Lelouard\*, Evelina Gatti\*, Fanny Cappello, Olivia Gresser, Voahirana Camosseto & Philippe Pierre

Centre d'Immunologie de Marseille-Luminy, CNRS-INSERM-Université Med., Campus de Luminy, Case 906, 13288 Marseille, Cedex 09, France

\* These authors contributed equally to this work

Dendritic cells (DCs) are antigen-presenting cells with the unique capacity to initiate primary immune responses<sup>1</sup>. Dendritic cells have a remarkable pattern of differentiation (maturation) that exhibits highly specific mechanisms to control antigen presentation restricted by major histocompatibility complex (MHC)<sup>2</sup>. MHC class I molecules present to CD8<sup>+</sup> cytotoxic T cells peptides that are derived mostly from cytosolic

proteins, which are ubiquitinated and then degraded by the proteasome<sup>3,4</sup>. Here we show that on inflammatory stimulation, DCs accumulate newly synthesized ubiquitinated proteins in large cytosolic structures. These structures are similar to, but distinct from, aggresomes and inclusion bodies observed in many amyloid diseases<sup>5,6</sup>. Notably, these dendritic cell aggresome-like induced structures (DALIS) are transient, require continuous protein synthesis and do not affect the ubiquitin–proteasome pathway. Our observations suggest the existence of an organized prioritization of protein degradation in stimulated DCs, which is probably important for regulating MHC class I presentation during maturation.

MHC class I presentation is linked directly to proteasome activity and consequently to cellular ubiquitinated protein levels<sup>7</sup>. To determine whether a principal regulation of MHC class I antigen presentation exists during DC maturation, we investigated whether protein ubiquitination was affected in these cells. We determined total protein ubiquitination levels in Langerhans cells (LCs) by confocal microscopy using the FK2 monoclonal antibody. FK2 is specific for mono- or polyubiquitinated proteins and, importantly,

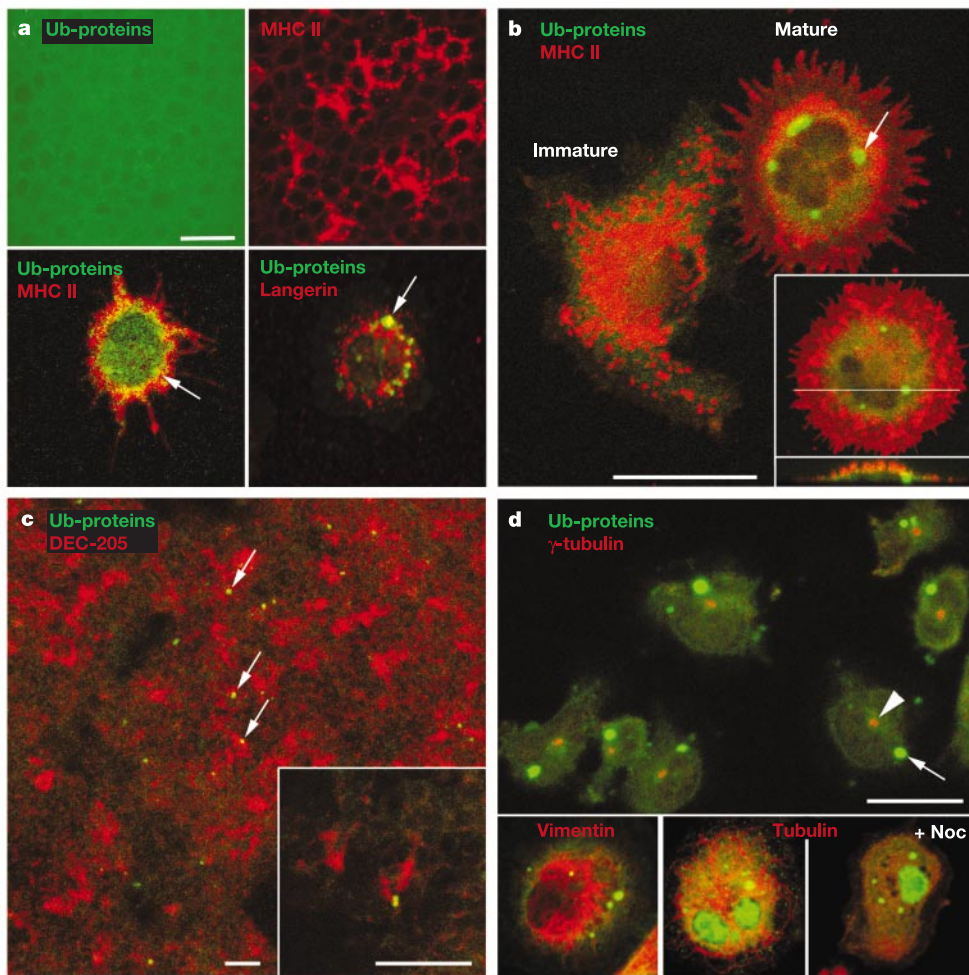


**Figure 1** Ubiquitinated protein accumulation during DC maturation. **a**, Explanted mouse epidermal sheets (top row) and emigrated Langerhans cells (bottom row) stained for ubiquitin conjugates (green), MHC class II or langerin (red), and visualized by confocal microscopy. Upon LPS treatment, LCs accumulated ubiquitinated proteins (Ub-proteins) in peripheral aggregates (arrows). **b**, Maturing human CD34<sup>+</sup>-derived LCs aggregated ubiquitinated proteins (green, indicated by an arrow), but not immature LCs, expressing HLA-DR (red) in lysosomal compartments. Z-sectioning revealed the circular shape of DALISs. **c**, In sections of mouse lymph node, only DCs (DEC-205 staining, in red)

accumulated ubiquitinated protein aggregates (green, indicated by arrows). Inset is a higher magnification image. **d**, Ubiquitinated protein aggregates (green; arrow) did not co-localize with the MTOC ( $\gamma$ -tubulin, in red and indicated by an arrowhead) in maturing mouse DCs derived from bone marrow, nor induce vimentin caging (red) in human LCs. Attempts to destabilize DALISs with nocodazole (Noc) were unsuccessful. The methanol fixation used to preserve microtubules (red) revealed nuclear ubiquitinated protein (large green patches). Scale bars, 20  $\mu$ m.

does not react with free ubiquitin<sup>8</sup>. We detected only weak cytosolic FK2 staining in mouse epidermal sheets (Fig. 1a), with no obvious co-localization with resident immature LCs. In contrast, we observed a strong accumulation of ubiquitinated proteins in mature emigrated LCs (Fig. 1a). Of note, in addition to slightly increased levels of soluble ubiquitinated substrates, FK2 staining revealed a strong peripheral aggregation of ubiquitinated material in most of the mature LCs, as shown by high cell-surface expression of MHC class II. We confirmed this observation in mature human CD34<sup>+</sup> precursor-derived LCs<sup>9</sup> in which ubiquitinated aggregates have a smooth and regular spherical shape and can reach a diameter of greater than 4  $\mu$ m (Fig. 1b and Z section). Most LCs contained only one principal aggregate, but their number could reach five per cell, a result also obtained with DCs derived from mouse bone marrow<sup>10</sup>.

In cryostat sections of mouse lymph node, most of the aggregate-containing cells also expressed the DC-specific lectin DEC-205 (ref. 11) (Fig. 1c). Aggregation of ubiquitinated proteins is therefore probably restricted to DCs and occurs during maturation both *in*

*vitro* and *in vivo*. Staining of other cell types (for example, B cells) did not show any aggregate formation on treatment with lipo-polysaccharide (LPS), suggesting further the DC specificity of the phenomenon (not shown).

Several examples of pathological aggregation of ubiquitinated proteins characteristic of amyloid diseases have been reported<sup>5</sup>. This phenomenon is also observed *in vitro* on pharmacological inhibition of the proteasome<sup>12–14</sup> or in cells transfected with mutated complementary DNAs<sup>15</sup>. These aggregates have been called aggresomes<sup>5</sup> and result from microtubule-dependent conglomeration of smaller aggregates in the area of the microtubule-organizing centre (MTOC)<sup>14,15</sup>. Aggresomes are surrounded by a cage formed by the intermediate filament protein vimentin<sup>14,15</sup>. As shown in Fig. 1d, FK2-positive aggregates did not co-localize with  $\gamma$ -tubulin (MTOC) nor vimentin. Dendritic-cell aggregate formation was not affected by the microtubule-depolymerizing drug nocodazole, indicating that these structures are distinct from 'classical' aggresomes observed under pathological circumstances. To underline this dis-

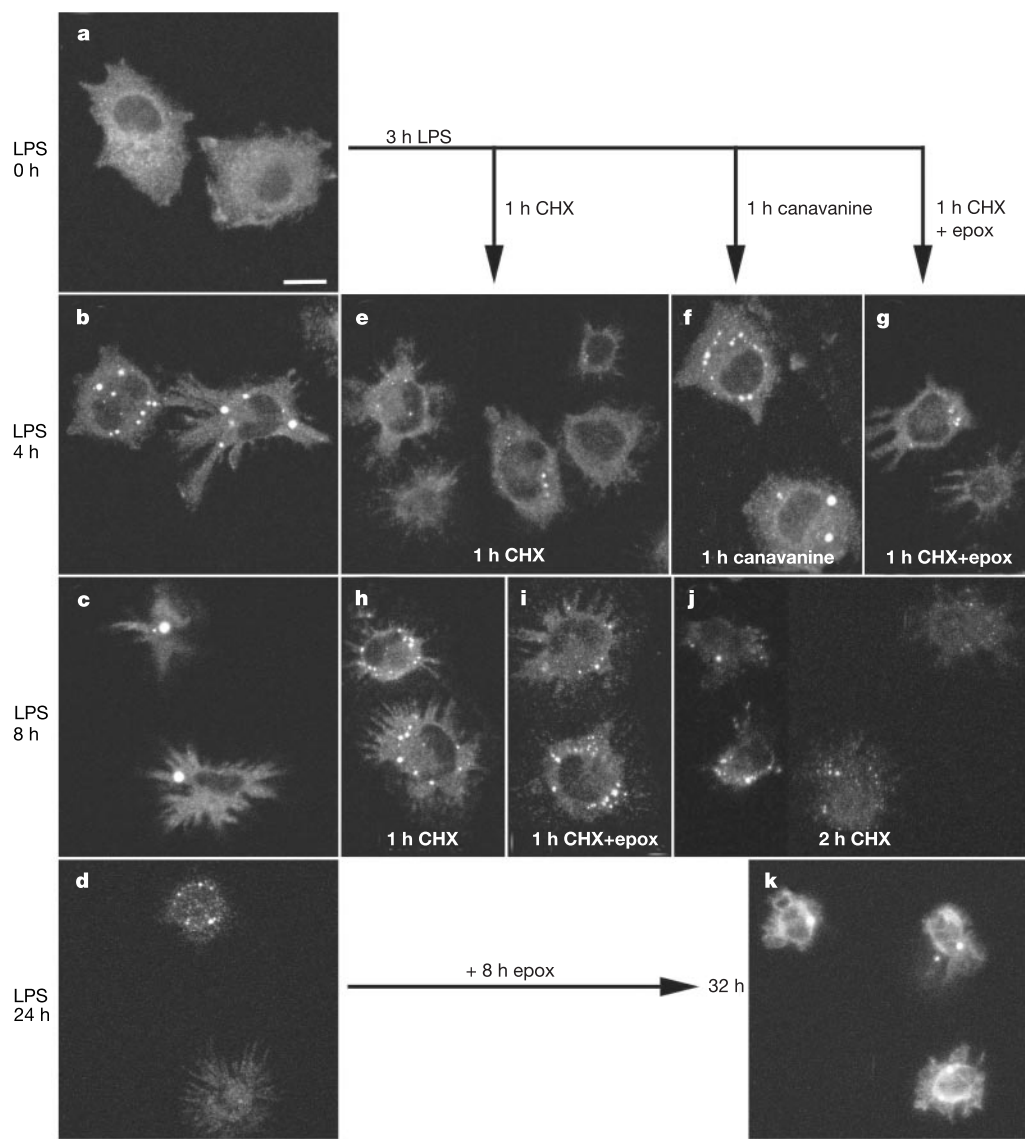


**Figure 2** DALIS formation is transient and depends on protein translation. Confocal microscopy was performed on maturing DCs derived from bone marrow to follow the kinetics of DALIS formation. **a–d**, DALIS appeared as early as 4 h after LPS stimulation, reached peak size at 8 h, and diminished in numbers and size at 24 h. **e–j**, One hour of cycloheximide (CHX) treatment prevented DALIS formation (**e**) or induced their

fragmentation at their peak size (**h, i**), whereas treatment with canavanine enhanced DALIS formation (**f**). Proteasome inhibition with epoxomicin (epox) did not counteract CHX treatment (**g, i**). **k**, At 24 h of maturation, incubation for a further 8 h with epoxomicin prevented DALIS disappearance. Scale bar, 10  $\mu$ m.

tinction, we name these aggregates 'DALIS', for dendritic cell aggresome-like inducible structures.

DALIS appeared as early as 4 h and peaked at around 8 h after LPS stimulation (Fig. 2a–c). After 24–36 h, most of the mature DCs no longer contained DALIS, and the average size of the remaining structures strongly diminished (Fig. 2d). DALIS are therefore transient, contrary to what has been observed for aggresomes.

An extremely high proportion of newly synthesized proteins represent defective ribosomal products (DRiPs), which are ubiquitinated and degraded shortly after synthesis<sup>16</sup>. DRiPs could therefore be an important part of material forming DALIS. We evaluated the contribution of newly synthesized proteins to DALIS formation using cycloheximide (CHX). A 1-h CHX treatment on maturing DCs prevented DALIS formation (Fig. 2e). Interestingly, inhibition of protein synthesis at a later maturation time (8 h) induced rapid DALIS fragmentation and often total disappearance after 2 h (Fig. 2h, j). The same happened also on anisomycin or emetine treatment, both of which are potent inhibitors of translation<sup>17</sup> (not shown). Protein synthesis is therefore required for the formation and the maintenance of the aggregate. To test whether DRiPs are

incorporated in DALIS, we incubated maturing DCs with the arginine analogue, canavanine. Canavanine causes synthesis of abnormal proteins (DRiPs), but unlike CHX, it does not inhibit translation<sup>13</sup>. Canavanine stimulated DALIS formation, indicating that aggregation requires functional translation but not necessarily intact proteins (Fig. 2f).

We used epoxomicin, a potent proteasome inhibitor<sup>18</sup>, to determine the contribution of proteolysis to DALIS fragmentation. Epoxomicin did not interfere with the disappearance of DALIS induced by CHX at early stages of maturation (Fig. 2g, i). The proteasome, which is inhibited after such treatment (Fig. 3), is therefore not involved directly in pharmacological destabilization of DALIS. On the contrary, epoxomicin treatment of mature DCs (24 h LPS) strongly enhanced accumulation of ubiquitinated proteins and re-formation of DALIS (Fig. 2k). The proteasome, therefore, participates actively in DALIS disappearance during late stages of maturation.

It has been suggested that aggresomes impair the ubiquitin–proteasome pathway, with potential cytotoxic effects in the case of neurodegenerative diseases<sup>19</sup>. To visualize a potential interference of

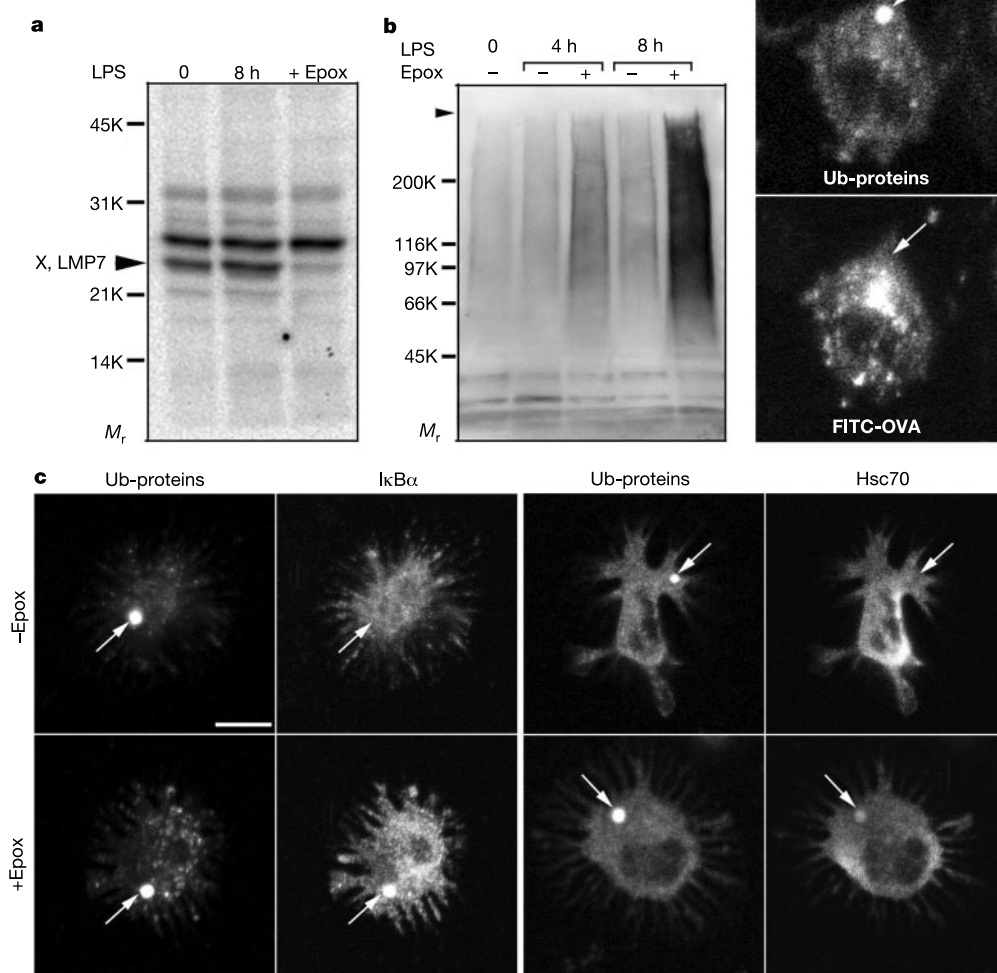


**Figure 3** Proteasome activity is not affected during DALIS formation and DCs can discriminate among ubiquitinated proteins. **a**, Proteasome activity, assessed by the active-site-directed probe <sup>125</sup>I-labelled NLVS, was similar in immature (lane 1) and maturing DCs (8 h LPS; lane 2). Pre-treatment for 1 h with epoxomicin inhibited subunits X and LMP7 of the proteasome (lane 3). **b**, Total ubiquitinated proteins, visualized by western blot with FK2, increased slightly during DC maturation. Proteasome inhibition

with epoxomicin led to the massive accumulation of ubiquitinated proteins. **c**, IkB $\alpha$  was not enriched in DALIS (arrows), except when epoxomicin was added (bottom of second column). The same was observed for Hsc70, a chaperone normally found in aggresomes (far right column). Scale bar, 10  $\mu$ m. **d**, Endocytosed FITC-ovalbumin was not enriched in DALIS after cytoplasmic translocation induced by CD40 ligation. Scale 1.4  $\times$  that in **c**.

DALISs with proteolysis, proteasome activity was evaluated by active site radioactive labelling. Incubation of DCs with the proteasome-specific probe  $^{125}\text{I}$ -labelled NLVS<sup>20</sup> (Fig. 3a) did not reveal any decrease in proteasome activity during maturation, contrary to the decreased activity observed on epoxomicin treatment. Furthermore, ubiquitinated protein accumulation in DCs treated with LPS for 4–8 h was strongly enhanced by epoxomicine, although LPS treatment alone provoked only a limited increase in ubiquitinated protein levels, as seen by immunoblotting (Fig. 3b). In conclusion, the proteasome seems to be functional in maturing DCs, and DALIS formation does not depend on nor seem to affect deeply its activity.

Efficient nuclear translocation of the transcription factor NF- $\kappa$ B, a necessary component of DC maturation<sup>21</sup>, requires ubiquitination and degradation of the phosphorylated  $\text{I}\kappa\text{B}\alpha$  chaperone protein.  $\text{I}\kappa\text{B}\alpha$  is therefore well suited to study the intracellular fate of ubiquitinated proteins during DC maturation. After 8 h of LPS stimulation, we did not observe any enrichment of  $\text{I}\kappa\text{B}\alpha$  in DALIS (Fig. 3c). Notably, pharmacological inhibition of the proteasome promoted accumulation in DALIS of  $\text{I}\kappa\text{B}\alpha$  as well as the heat shock protein Hsc70 (Fig. 3c).  $\text{I}\kappa\text{B}\alpha$  is therefore normally degraded in maturing DCs, which seem to be able to discriminate among different ubiquitinated proteins during DALIS formation. Aggregated proteins are likely to be more resistant to proteolysis, and DCs could prioritize selected ubiquitinated protein degradation (for

example,  $\text{I}\kappa\text{B}$ ) by not storing them in DALIS. However, DALIS aggregation specificity can be abrogated by epoxomicin treatment. The exclusion from DALIS of Hsc70, a molecule normally found in aggresomes<sup>5</sup>, further supports the distinction between these two types of structure.

We investigated the fate of endocytosed proteins during translocation from the endocytic pathway to the cytosol. This transport pathway seems to be DC specific and is required for cross-presentation<sup>22</sup>. After fluorescein isothiocyanate (FITC)-conjugated ovalbumin uptake, DCs were activated with CD40 ligation to induce maturation. Although under these conditions DALIS formation occurred normally, no selective enrichment of cytosolic FITC-ovalbumin was detected (Fig. 3d). Translocated proteins are therefore not specifically targeted to the aggregates, further supporting the existence of selective protein degradation during early DC maturation.

FK2 detects a large pool of cytosolic and nuclear ubiquitinated proteins (Figs 1d and 3b). We adapted a nuclear matrix protein isolation procedure<sup>23</sup> to partially purify DALIS by extracting contaminating cytosolic and nuclear ubiquitinated material. DALIS resisted sequential extractions with Triton-X100, DNase I and 2 M NaCl, whereas most other ubiquitin-conjugated material was eliminated under such conditions (see Supplementary Information). We used the FK1 antibody, specific for polyubiquitinated proteins<sup>8</sup>, to demonstrate that DALIS contain polyubiquitinated conjugates,

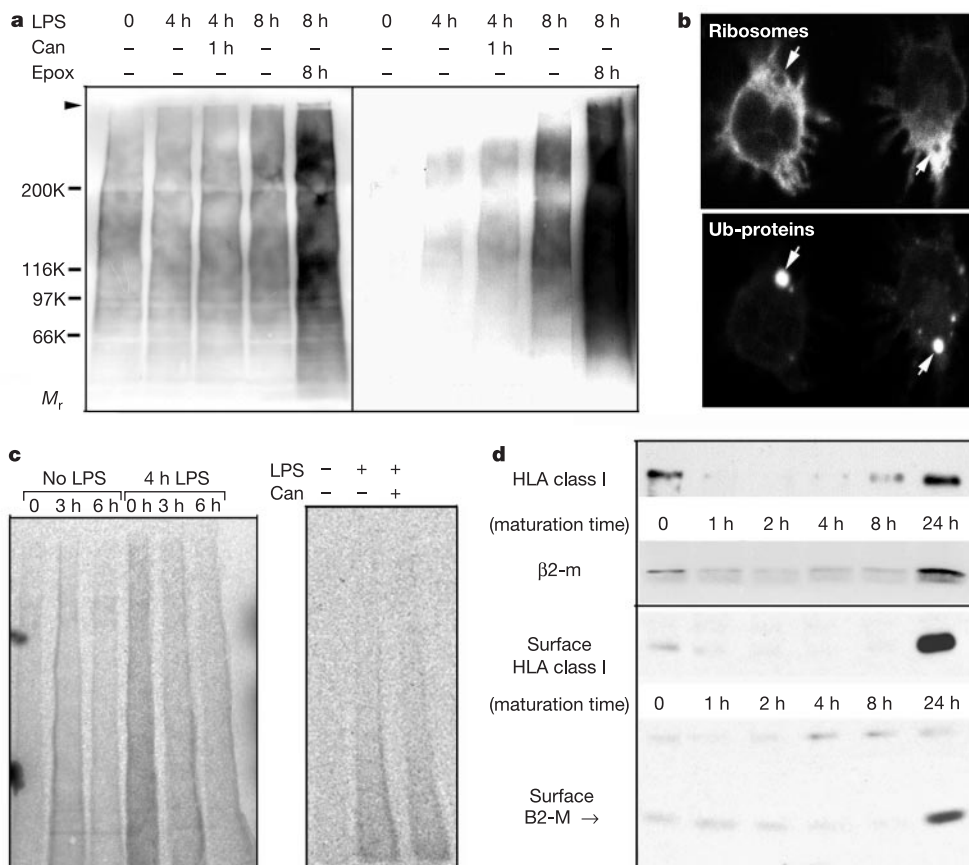


**Figure 4** Newly synthesized proteins are targeted to DALIS. **a**, Immature, maturing (4 h and 8 h LPS), canavanine- (can), or epoxomicin-treated DCs were submitted to biochemical extraction, SDS-PAGE and FK2 immunolabelling. Triton-X100 soluble fractions are shown on the left and 2 M NaCl non-extractable material enriched for DALIS are on the right. **b**, Ribosomes (top) are enriched in the vicinity of DALIS (bottom) in maturing DCs. Scale is the same as in Fig. 3c. **c**, Immature and maturing DCs with or without stimulation by LPS for 4 h were pulse-labelled with  $^{35}\text{S}$ -labelled Promix (left) or

$^{35}\text{S}$ -labelled cysteine (right) for 5 min, and chased for the indicated times, before selective extraction and FK2 immunoprecipitation. **d**, Immunoprecipitation from human LCs of HLA class I with W6/32 (top), or surface biotinylated complexes with B9.12.1 (bottom) at different times of maturation, induced either by TNF- $\alpha$  (top) or bacteria (bottom). Immunoprecipitated material (heavy chain and  $\beta 2$ -microglobulin;  $\beta 2\text{-m}$ ) was revealed by immunoblot with specific antibodies or anti-biotin.

whereas most nuclear ubiquitinated proteins are monoconjugated<sup>13</sup>. Interestingly, the level of detergent-soluble ubiquitinated proteins detected by immunoblot was unaffected by DC maturation, suggesting that a large increase in ubiquitinated material does not promote DALIS formation (Fig. 4a, left). After selective enrichment, ubiquitinated proteins were found only in the insoluble material of maturing DCs (Fig. 4a, right). The smearable appearance and the overall molecular mass pattern indicated that an array of proteins is incorporated in DALIS. Epoxomicin treatment induced abnormal accumulation of ubiquitinated proteins both in soluble and insoluble DC fractions. Importantly, induction of DRiPs by a 1-h canavanine treatment significantly increased the abundance of insoluble ubiquitinated material in maturing DCs, whereas the Triton-X100 soluble pool was unchanged (Fig. 4a). This last piece of evidence confirms that DRiPs are incorporated into DALIS.

To further investigate DRiP incorporation into DALIS, we performed radioactive pulse-chase experiments. After selective extraction, the ubiquitinated material was immunoprecipitated with FK2 before separation and autoradiography (Fig. 4c, left). High levels of insoluble radioactivity were found already in maturing DCs after a short pulse (5 min), indicating that newly synthesized proteins were immediately ubiquitinated and rapidly targeted to DALIS. Furthermore, immunoprecipitated ubiquitinated proteins were relatively long lived as they could still be detected after 6 h of chase. As expected, immature DCs did not display this type of rapid aggregation; however, radioactive ubiquitinated proteins could be immunoprecipitated from insoluble fractions after 3 h of chase. At that time, maturation and subsequent DALIS formation were induced by <sup>35</sup>S-labelled Promix, most probably contaminated by endotoxin (not shown). To rule out the possibility that the observed labelling could be due to incorporation of <sup>35</sup>S into ubiquitin only, a 5-min pulse was performed with <sup>35</sup>S-labelled cysteine, an amino acid absent from the ubiquitin molecule (Fig. 4c, right). Ubiquitinated proteins tagged with <sup>35</sup>S-labelled cysteine aggregated rapidly in maturing DCs, demonstrating that newly translated proteins, conjugated to pre-existing ubiquitin, can form DALIS. In agreement with the DRiP hypothesis, aggregation of radioactive proteins also occurred in maturing DCs pre-treated with canavanine.

The extreme rapidity with which newly synthesized proteins are incorporated into DALIS led us to investigate whether the ribosomal machinery was affected during DALIS formation. Ribosomes, detected by an antibody specific for the S6 ribosomal protein, were enriched in rings surrounding the aggregates. In extreme cases, the translation apparatus was almost completely redistributed in the vicinity of DALIS (Fig. 4b). This marked phenomenon could explain the rapidity of DRiP incorporation into DALIS, and suggests that it might happen along with translation.

The direct link between protein translation, DRiPs and MHC class-I-restricted presentation has been demonstrated by several laboratories using different techniques<sup>16,24,25</sup>. DRiPs are considered as the main source for MHC class-I-restricted antigenic peptides in both professional (that is, DCs, B cells, macrophages) and non-professional (that is, epithelial/endothelial cells) antigen-presenting cells. We therefore investigated MHC class I-peptide complex assembly in maturing LCs, on which DALIS occurrence should have an impact. W6/32 and B9.12.1 are antibodies used to detect assembled human heterotrimeric complexes formed by  $\beta 2$ -microglobulin, class I heavy chain and peptide<sup>26</sup>. The amount of immunoprecipitated molecules reflects the activity of the HLA class I presentation pathway at a given time. In maturing CD34<sup>+</sup>-derived human LCs, class I heavy chain and  $\beta 2$ -microglobulin immunoprecipitated by W6/32 were lost rapidly, before a major increase after 24 h (Fig. 4d, top). This late increase was probably due to enhanced transcription and translation of HLA genes<sup>27</sup>. The rapid loss of reactivity indicated a high turnover of the class I complexes and an overall reduction of its formation on stimulation. Loss of

W6/32 epitopes correlated strongly with the kinetics of DALIS formation (Fig. 2). HLA class I assembly and loading seem therefore dependent on DRiP storage, and probably result from a biochemical event occurring very rapidly after stimulation. This regulation also involves the rapid disassembly of pre-existing surface heteromeric complexes, as shown by immunoprecipitation of biotinylated surface molecules with B9.12.1 in bacteria-stimulated LCs (Fig. 4d, bottom).

Until now, observation of large protein aggregates *in vivo* was limited to pathological situations. We show here that reversible ubiquitinated protein aggregation occurs in a normal physiological context. We demonstrate that this aggregation is DC specific and inducible by inflammatory stimuli. DALIS formation could be the result of a massive increase in the total level of ubiquitination during maturation with a saturating effect on the proteasome. Our data do not support this hypothesis, however, as little difference in the total ubiquitinated protein pool is found between immature and maturing DCs. Furthermore, if DALIS were the result of a mere saturation of the proteasome-ubiquitin degradation pathway, molecules such as I $\kappa$ B $\alpha$  should be enriched in these structures as observed when proteolysis is inhibited with epoxomicin. Although the mechanism of DALIS formation is still unclear, we have determined that a constant flow of newly synthesized proteins, likely to be DRiPs, supports the growth of these structures. The relatively long half-life of insoluble polyubiquitinated proteins and the constant enlargement of DALIS for at least 8 h suggest that DRiPs are poorly degraded at the onset of DC maturation. The speed of the ubiquitination and aggregation process implies the existence of a specific sorting machinery dedicated to DALIS formation, to which ribosomes might physically participate.

By limiting DRiP degradation, maturing DCs might have the ability to control MHC class I loading and peptide presentation<sup>28</sup>. This hypothesis is strongly supported by the rapid decrease in W6/32 and B9.12.1 epitopes observed at early stages of maturation. This drop probably reflects a change in peptide availability for MHC loading, with potential consequences on antigen presentation by DCs, as well as on their role in establishing tolerance and immunity<sup>29</sup>. DALIS could also represent antigen storage structures. The precise timing of DALIS formation could allow the coordination of MHC class I and class II processing at DC arrival in lymph nodes. □

## Methods

### Materials and cell culture

We purchased all chemicals from Sigma unless stated otherwise. Epoxomicin was purchased from Affinity.

Male C57/BL6 mice (7–8 weeks of age) were purchased from Charles River Laboratories. Bone-marrow-derived DCs and epidermal sheets were cultured as described previously<sup>10</sup>. Human Langerhans cells were obtained as described<sup>9</sup> and matured with tumour-necrosis factor- $\alpha$  (Preprotech) or *Escherichia coli*.

### Antibodies and immunocytochemistry

We performed immunofluorescence confocal microscopy with Leica TCS 4D as described<sup>10</sup>. Murine I-A was detected using the 'Rivoli' affinity-purified rabbit polyclonal antibody<sup>10</sup>. Human HLA class I and II were detected using anti-heavy-chain and anti-DR rabbit polyclonal antibody, respectively (gift of J. Neefjes). Polyclonal anti-tubulin and  $\gamma$ -tubulin were a gift of T. Kreis and M. Bornman. Rat monoclonal NLDC-145 anti-DEC205 was obtained from R. Steinman, and rabbit polyclonal anti-langerin was a gift of S. Sealand. Monoclonal antibodies FK1, FK2 and polyclonal antibody against ubiquitin were obtained from Affinity. Anti-I $\kappa$ B $\alpha$  and anti-Hsc70 were obtained from Santa-Cruz. Anti- $\beta$ 2-ribosomal protein was obtained from Cell Signaling Technology. Anti- $\beta$ 2-microglobulin, W6/32 and B9.12.1 were from Biodesign. All secondary antibodies were from Immunotech. For pharmacological treatments, cells were incubated respectively with 1  $\mu$ M epoxomicin, 15 mM canavanine or 25  $\mu$ M CHX. Dendritic cells were incubated with FITC-OVA (10  $\mu$ g ml<sup>-1</sup>) for 4 h before CD40 ligation with rat anti-mouse CD40 antibody (FSK45) for an additional 4 h.

### Proteasome catalytic subunit labelling

Specific proteasome active-site inhibitor NLVS (gift of H. Ploegh) was iodinated using the iodogen method as reported previously<sup>20</sup>. Immature and maturing DCs (7 h LPS), pre-treated or not with 1  $\mu$ M epoxomicin (1 h), were incubated for 1 h with <sup>125</sup>I-labelled NLVS at 37°C, and washed twice with PBS before lysis in sample buffer and 15% SDS-polyacrylamide gel electrophoresis analysis.

## Selective enrichment of DALIS

Nocodazole-treated DCs were submitted to a 30-min 1% Triton-X100 extraction at 4°C before a 30-min DNase I (100 µg ml<sup>-1</sup>) treatment at 37°C in 20 mM Tris pH 7.4, 1.5 mM MgCl<sub>2</sub>, 10 mM NaCl. Nuclear material extraction was performed for 30 min at 4°C with a solution of 20 mM Tris pH 7.4, 1.5 mM MgCl<sub>2</sub>, 2 M NaCl. Remaining material was washed with PBS and submitted to immunocytochemical and biochemical analysis.

## Radiolabelling, immunoprecipitation and immunoblots

Roughly 2 × 10<sup>7</sup> DCs were pulse-labelled with 10 mCi ml<sup>-1</sup> <sup>35</sup>S-labelled Promix or <sup>35</sup>S-labelled cysteine (both from Amersham Pharmacia Biotech) in labelling medium for 5 min, and chased for various time at 37°C as described<sup>10</sup>. Radiolabelled DALIS-enriched samples were solubilized at 95°C for 5 min in SDS 1% before dilution in 10 mM Tris, 150 mM NaCl (pH 7.4) containing 1% Triton-X100, 1 µM epoxomicin and protease inhibitor cocktail. Samples were pre-cleared with protein A Sepharose (Amersham Pharmacia Biotech) at 4°C and immunoprecipitated overnight with the FK2 antibody. Immunoprecipitates were analysed onto 2–10% gradient SDS-PAGE gels and quantified with a Fuji phosphorimager. Immunoprecipitations with W6/32 and B9.12.1 (after surface biotinylation) were performed as described<sup>10</sup> for 2 h at 4°C before immunoblot analysis. Immunoblots were performed after transfer on Immobilon P (Millipore) and detected by chemiluminescence (Amersham Pharmacia Biotech).

Received 28 December 2001; accepted 19 February 2002.

1. Banchereau, J. & Steinman, R. M. Dendritic cells and the control of immunity. *Nature* **392**, 245–252 (1998).
2. Mellman, I. & Steinman, R. M. Dendritic cells: specialized and regulated antigen processing machines. *Cell* **106**, 255–258 (2001).
3. Hirsch, C. & Ploegh, H. L. Intracellular targeting of the proteasome. *Trends Cell Biol.* **10**, 268–272 (2000).
4. Yewdell, J. W. & Bennink, J. R. Cut and trim: generating MHC class I peptide ligands. *Curr. Opin. Immunol.* **13**, 13–18 (2001).
5. Kopito, R. R. Aggresomes, inclusion bodies and protein aggregation. *Trends Cell Biol.* **10**, 524–530 (2000).
6. Sherman, M. Y. & Goldberg, A. L. Cellular defenses against unfolded proteins: a cell biologist thinks about neurodegenerative diseases. *Neuron* **29**, 15–32 (2001).
7. Weissman, A. M. Themes and variations on ubiquitylation. *Nature Rev. Mol. Cell. Biol.* **2**, 169–178 (2001).
8. Fujimuro, M., Sawada, H. & Yokosawa, H. Production and characterization of monoclonal antibodies specific to multi-ubiquitin chains of polyubiquitinated proteins. *FEBS Lett.* **349**, 173–180 (1994).
9. Gatti, E. *et al.* Large-scale culture and selective maturation of human Langerhans cells from granulocyte colony-stimulating factor-mobilized CD34<sup>+</sup> progenitors. *J. Immunol.* **164**, 3600–3607 (2000).
10. Pierre, P. *et al.* Developmental regulation of MHC class II transport in mouse dendritic cells. *Nature* **388**, 787–792 (1997).
11. Jiang, W. *et al.* The receptor DEC-205 expressed by dendritic cells and thymic epithelial cells is involved in antigen processing. *Nature* **375**, 151–155 (1995).
12. Wojcik, C., Schroeter, D., Wilk, S., Lamprecht, J. & Paweletz, N. Ubiquitin-mediated proteolysis centers in HeLa cells: indication from studies of an inhibitor of the chymotrypsin-like activity of the proteasome. *Eur. J. Cell. Biol.* **71**, 311–318 (1996).
13. Anton, L. C. *et al.* Intracellular localization of proteasomal degradation of a viral antigen. *J. Cell. Biol.* **146**, 113–124 (1999).
14. Johnston, J. A., Ward, C. L. & Kopito, R. R. Aggresomes: a cellular response to misfolded proteins. *J. Cell. Biol.* **143**, 1883–1898 (1998).
15. Garcia-Mata, R., Bebok, Z., Sorscher, E. J. & Sztul, E. S. Characterization and dynamics of aggresome formation by a cytosolic GFP-chimera. *J. Cell. Biol.* **146**, 1239–1254 (1999).
16. Schubert, U. *et al.* Rapid degradation of a large fraction of newly synthesized proteins by proteasomes. *Nature* **404**, 770–774 (2000).
17. Iordanov, M. S. *et al.* Ribotoxic stress response: activation of the stress-activated protein kinase JNK1 by inhibitors of the peptidyl transferase reaction and by sequence-specific RNA damage to the alpha-sarcin/ricin loop in the 28S rRNA. *Mol. Cell. Biol.* **17**, 3373–3381 (1997).
18. Meng, L. *et al.* Epoxomicin, a potent and selective proteasome inhibitor, exhibits *in vivo* anti-inflammatory activity. *Proc. Natl. Acad. Sci. USA* **96**, 10403–10408 (1999).
19. Bene, N. E., Sampat, R. M. & Kopito, R. R. Impairment of the ubiquitin-proteasome system by protein aggregation. *Science* **292**, 1552–1555 (2001).
20. Bogyo, M., Shin, S., McMaster, J. S. & Ploegh, H. L. Substrate binding and sequence preference of the proteasome revealed by active-site-directed affinity probes. *Chem. Biol.* **5**, 307–320 (1998).
21. Rescigno, M., Martino, M., Sutherland, C. L., Gold, M. R. & Ricciardi-Castagnoli, P. Dendritic cell survival and maturation are regulated by different signalling pathways. *J. Exp. Med.* **188**, 2175–2180 (1998).
22. Thery, C. & Amigorena, S. The cell biology of antigen presentation in dendritic cells. *Curr. Opin. Immunol.* **13**, 45–51 (2001).
23. Staufenbiel, M. & Deppert, W. Preparation of nuclear matrices from cultured cells: subfractionation of nuclei *in situ*. *J. Cell Biol.* **98**, 1886–1894 (1984).
24. Reits, E. A., Vos, J. C., Gromme, M. & Neefjes, J. The major substrates for TAP I are derived from newly synthesized proteins. *Nature* **404**, 774–778 (2000).
25. Khan, S. *et al.* Neosynthesis is required for the presentation of a T cell epitope from a long-lived viral protein. *J. Immunol.* **167**, 4801–4804 (2001).
26. Brodsky, F. M. & Parham, P. Monomorphic anti-HLA-A,B,C monoclonal antibodies detecting molecular subunits and combinatorial determinants. *J. Immunol.* **128**, 129–135 (1982).
27. Huang, Q. *et al.* The plasticity of dendritic cell responses to pathogens and their components. *Science* **294**, 870–875 (2001).
28. Yewdell, J. W., Schubert, U. & Bennink, J. R. At the crossroads of cell biology and immunology: DRiPs and other sources of peptide ligands for MHC class I molecules. *J. Cell. Sci.* **114**, 845–851 (2001).
29. Hawiger, D. *et al.* Dendritic cells induce peripheral T cell unresponsiveness under steady state conditions *in vivo*. *J. Exp. Med.* **194**, 769–779 (2001).

Supplementary Information accompanies the paper on *Nature*'s website (<http://www.nature.com>).

## Acknowledgements

We thank A.-M. Imbert, C. Chabannon and all the personnel at the cell repository of the Centre de Thérapie Cellulaire (Institut Paoli-Calmettes) for providing access to human CD34<sup>+</sup> cells. We also thank J. Yewdell, P. Machy and L. Delamarre for a gift of antibody and for discussions. This work is supported by grants to P.P. from the Ministère de la Recherche et de la Technologie (Action Concertée Initiative Blanche), the Association pour la Recherche contre le Cancer, and the Fondation Schlumberger pour l'Education et la Recherche. H.L. is supported by a Sidaction and Agence Nationale de Recherches sur la Sida fellowships, and E.G. is an EU Marie Curie fellow.

## Competing interests statement

The authors declare that they have no competing financial interests.

Correspondence and requests for materials should be addressed to P.P. (e-mail: pierre@ciml.univ-mrs.fr).

## Identification of a factor that links apoptotic cells to phagocytes

Rikinari Hanayama\*†, Masato Tanaka\*†, Keiko Miwa\*†, Azusa Shinohara‡, Akihiro Iwamatsu‡ & Shigekazu Nagata\*†

\* Department of Genetics, Osaka University Medical School, † Core Research for Evolutional Science and Technology, Japan Science and Technology Corporation, 2-2 Yamada-oka, Suita, Osaka, 565-0871, Japan

‡ Central Laboratories for Key Technology, Kirin Brewery Co., Ltd, 1-13-5 Fukuura, Kanazawa, Yokohama, Kanagawa 236-0004, Japan

Apoptotic cells are rapidly engulfed by phagocytes to prevent the release of potentially noxious or immunogenic intracellular materials from the dying cells, thereby preserving the integrity and function of the surrounding tissue<sup>1</sup>. Phagocytes engulf apoptotic but not healthy cells, indicating that the apoptotic cells present a signal to the phagocytes, and the phagocytes recognize the signal using a specific receptor<sup>2</sup>. Here, we report a factor that links apoptotic cells to phagocytes. We found that milk fat globule-EGF-factor 8 (MFG-E8)<sup>3,4</sup>, a secreted glycoprotein, was produced by thioglycollate-elicited macrophages. MFG-E8 specifically bound to apoptotic cells by recognizing aminophospholipids such as phosphatidylserine. MFG-E8, when engaged by phospholipids, bound to cells via its RGD (arginine-glycine-aspartate) motif—it bound particularly strongly to cells expressing  $\alpha_v\beta_3$  integrin. The NIH3T3 cell transformants that expressed a high level of  $\alpha_v\beta_3$  integrin were found to engulf apoptotic cells when MFG-E8 was added. MFG-E8 carrying a point mutation in the RGD motif behaved as a dominant-negative form, and inhibited the phagocytosis of apoptotic cells by peritoneal macrophages *in vitro* and *in vivo*. These results indicate that MFG-E8 secreted from activated macrophages binds to apoptotic cells, and brings them to phagocytes for engulfment.

Cells expressing a caspase-resistant ICAD (inhibitor of caspase-activated DNase) do not undergo apoptotic DNA fragmentation, but their DNA can still be cleaved when the cells are phagocytosed by macrophages<sup>5</sup>. This system was used to examine the phagocytosis of apoptotic cells. As shown in Fig. 1a, when thymocytes from transgenic mice carrying caspase-resistant ICAD mutant (ICAD-Sdm)<sup>5</sup> were treated with dexamethasone, about 50% of the cells became annexin-V-positive within 4 h, but they were not stained by TUNEL (TdT-mediated dUTP nick end labelling). Co-culture of macrophages with apoptotic thymocytes, but not with freshly